Histol Histopathol (2023) 38: 185-197

http://www.hh.um.es

Histology and Histopathology
From Cell Biology to Tissue Engineering

ORIGINAL ARTICLE **Open Access**

Circ_0000467 regulates proliferation, migration, invasion, and apoptosis in gastric cancer by targeting the miR-622/ROCK2 axis

Shengquan Tan[1]*, Lingbo Hu[1]*, Rui Lei[1], Ruo Wang[1] and Jiaquan Chen[2]

[1]Department of Health Management Center and [2]Department of Oncology, The Central Hospital of Enshi Tujia and Miao Autonomous Prefecture, Enshi City, Hubei Province, China.

*These authors contributed equally to this paper

Summary. Background. Gastric cancer (GC) ranks fourth as a cause of cancer-induced mortality worldwide. Recently, some studies have demonstrated that circular RNAs (circRNAs) play vital roles in human cancers, including GC.

Methods. The expression levels of circ_0000467, microRNA-622 (miR-622), and Rho-associated coiled-coil-containing protein kinase2 (ROCK2) were determined by RT-qPCR assay. The protein expression was quantified by western blot assay. The interaction relationship between miR-622 and circ_0000467 or ROCK2 was confirmed by dual-luciferase reporter assay and RIP assay. The biological behaviors of GC cells including proliferation, apoptosis, migration, and invasion were determined by EdU assay, colony-forming assay, flow cytometry, and transwell assay. The effects of circ_0000467 silencing *in vivo* were assessed by a xenograft experiment in nude mice.

Results. MiR-622 was downregulated and ROCK2 was upregulated in GC tissues and cells. Loss-of-function experiment revealed that overexpression of miR-622 decreased proliferation, migration, and invasion while it increased apoptosis in GC cells. Furthermore, ROCK2 was a functional target of miR-622, and upregulation of ROCK2 abolished miR-622-induced effects on GC cells. What's more, circ_0000467 was upregulated in GC, and inhibition of miR-622 reversed silencing of circ_0000467-caused effects on GC cells, suggesting that miR-622 was a target of circ_0000467. The suppression of circ_0000467 was able to slow the tumor growth *in vivo*.

Conclusion. Mechanistically, circ_0000467 functioned as an oncogenic regulator in GC by specifically binding to miR-622 to upregulate ROCK2, which might be novel diagnostic markers for GC.

Key words: Gastric cancer, circ_0000467, miR-622, ROCK2

Introduction

Gastric cancer (GC), a common malignant tumor that occurs in the digestive system, is a major reason of tumor-associated death worldwide; besides, GC is fifth most frequently diagnosed cancer with high incidence (Correa, 2013; Bray et al., 2018). Although technological development have made a significant contribution to the diagnosis and treatment of GC, patients with GC may still suffer from a poor clinical outcome (Song et al., 2017; Li et al., 2020). Consequently, it is important to look into molecular mechanism and new biomarkers of GC.

Circular RNAs (circRNAs) are a new type of RNA with a closed continuous loop structure (Li et al., 2020). Although circRNA is without a 5'end cap or a 3'terminal poly (A) tail structure, it is confirmed to play a vital role in human cancers, including GC (Li et al., 2020). For example, Lu et al. reported that circ-RanGAP1 could promote invasion and metastasis of GC by targeting miR-877-3p (Lu et al., 2020). Circ_0000467 is derived from spindle and kinetochore associated complex subunit 3 (SKA3) gene and is located on chr13 (21742126-21742538). Interestingly, the diagnostic and prognostic value of circ_0000467 were revealed in GC, suggesting that circ_0000467 was a potential therapeutic target for GC (Lu et al., 2019). Therefore, the functional effects of circ_0000467 were investigated in GC.

MicroRNAs (miRNAs) are small RNAs with a length of about 20-24 nucleotides (Saliminejad et al., 2019). Previous reports also evidenced that aberrant expression of miR-622 was frequently reported in

Corresponding Author: Jiaquan Chen, Department of Oncology, The Central Hospital of Enshi Tujia and Miao Autonomous Prefecture, No.158 Wuyang Avenue, Enshi 445000, Hubei Province, China. e-mail: chenjiaquanes@126.com

DOI: 10.14670/HH-18-508

multiple human malignancies, including glioma (Xu et al., 2018), breast cancer (Liu et al., 2019a), and colorectal cancer (Fang et al., 2019), indicating that miR-622 might function as a cancer inhibitor. More importantly, miR-622 expression was significantly connected to cellular invasion and tumor metastasis in GC (Guo et al., 2011). We hypothesized that miR-622 could regulate the malignant behaviors of GC cells.

Rho-associated coiled-coil-containing protein kinase2 (ROCK2), a member of the ROCK family, plays an important role in organization of the actin cytoskeleton, which is involved in cell adhesion, movement, and proliferation (Julian and Olson, 2014; Wei et al., 2016). A previous report showed that ROCK2 overexpression was associated with poor prognosis of breast cancer patients (Yi et al., 2018). Moreover, Sun et al. have reported that miR-4529-5p can regulate proliferation and invasion of GC cells, which is closely associated with ROCK2 expression (Sun et al., 2019). Thus, the regulatory roles of ROCK2 were investigated in GC.

In the view of the above studies, we measured the abundance of circ_0000467, miR-622, and ROCK2 in GC in this study. Additionally, we hypothesized that circ_0000467 could regulate malignant phenotypes of GC cells by being implicated in miR-622 and ROCK2 expression.

Materials and methods

Patient specimens

Surgically resected GC tissues and adjacent non-tumorous tissues were collected from 41 GC patients at the central hospital of enshi tujia and miao autonomous prefecture. The collected tissues were timely frozen in liquid nitrogen and maintained in -80°C for subsequent study. In addition, a part of the fresh tissue was prepared into paraffin sections, and then the tissue was stained with ROCK2 antibody (#9029S; 1:50 dilution, CST, Danvers, MA, USA) to perform immunohistochemical (IHC) staining according to the instructions of the SP kit (Solarbio, Beijing, China). All participants had not received preoperative treatments before surgical resection and completed the written informed consents. This study was authorized by the Ethics Committee of the central hospital of enshi tujia and miao autonomous prefecture.

Cell lines and cell culture

Human gastric mucosal cells (GES-1) and GC cell lines (HGC-27, AGS, and NUGC3) were procured from Chinese Academy of Sciences (Shanghai, China). These cells were propagated in DMEM medium (Biochrom KG, Berlin, Germany) supplemented with 10% (v/v) FBS (Thermo Fisher Scientific, Waltham, MA, USA) in an atmosphere of 37°C and 5% CO_2.

RNA isolation and RT-qPCR

TriQuick Reagent kit (Thermo Fisher Scientific) was used for RNA extraction in compliance with manufacturer's instructions. PrimeScript reverse transcriptase reagent kit (Vazyme, Nanjing, China) was used to synthesize cDNA. RT-qPCR assay was carried out using 2×SYBR-Green buffer (Thermo Fisher Scientific), complementary DNA, specially primers, and nuclease-free water in 10 μL of reaction mixture under Roche LC480 system (Roche Applied Science, Mannheim, Germany). GAPDH was used as an endogenous control for circ_0000467 and ROCK2, while small nuclear RNA U6 was used for miR-622 based on the $2^{-\Delta\Delta Ct}$ method. The sequences of primers are shown below: circ_0000467 (up 5'-GGGACTTAAAAATGCGAGGA-3'; down 5'-GCAACAGGAGGATCAGACAGA-3'); miR-622 (up 5'-GCCGAGACAGTCTGCTGAGGT-3'; down 5'-CCAGTGCAGGGTCCGAGGT-3'); ROCK2 (up 5'-TCAGAGGTCTACAGATGAAGGC-3'; down 5'-CCAGGGGCTATTGGCAAAGG-3'); SKA3 (up 5'-TACACGAGCAAGAAGCCATTAAC-3'; down 5'-GGATACGATGTACCGCTCAAGT-3'); GAPDH (up 5'-CTCTGCTCCTCCTGTTCGAC-3'; down 5'-CGACCAAATCCGTTGACTCC-3'); U6 (up 5'-CTCGCTTCGGCAGCACATA-3'; down 5'-CGAATTTGCGTGTCATCCT-3').

Western blot assay

GC cells or tissues were lysed in ice-cold RIPA lysis buffer (Beyotime, Shanghai, China). After quantifying by BCA protein assay kit (Pierce, Rockford, MA, USA), 50 μg of protein was fractionated by SDS-PAGE gel and then shifted onto PVDF membranes (Bio-Rad, Hercules, CA, USA). Subsequently, membranes were blocked by 5% skim milk powder and then incubated with primary antibody at 4°C overnight, including BCL2-Associated X (Bax; #5023S; 1:1500 dilution), Matrix Metallopeptidase 9 (MMP9; #13667S; 1:1500 dilution), ROCK2 (#9029S; 1:1500 dilution), and GAPDH (#2118S; 1:2500 dilution; all purchased from CST). Then secondary antibodies Anti-rabbit IgG (#7074S; 1:2000 dilution; CST) were added into the membranes and incubated for 1h at room temperature. The blots were visualized using a Clarity™ Western ECL Substrate Kit (Bio-Rad).

Transfection assay

Transfection of oligonucleotide and plasmid was conducted by Lipofectamine 2000 (Thermo Fisher Scientific). The mimic of miR-622 and negative control (miR-622 and miR-NC), inhibitor of miR-622 and negative control (in-miR-622 and in-miR-NC), interfering RNA (siRNA) scrambled control (si-NC) and siRNA targeting circ_0000467 (si-circ_0000467#1/

#2/#3) were synthesized by RiboBio (Shanghai, China) and 100 μM was used for each transfection. ROCK2-overexpression vector (ROCK2) and empty vector (pcDNA) were designed by Sangon (Shanghai, China). For plasmid transfection, the final concentration was 1 μg/mL. GC cells were harvested at 48h post-transfection and transfection efficacy was investigated by RT-qPCR assay.

Dual-luciferase reporter assay

The targets of circ_0000467 and miR-622 were predicted by circinteractome (https://circinteractome.nia.nih.gov/mirna_target_sites.html) and targetscan (http://www.targetscan.org/vert_71/), respectively. The wild type and mutant sequences of circ_0000467 or 3' untranslated region (UTR) of ROCK2 mRNA containing the miR-622 interacted sequence were generated by PCR amplification and inserted into reporter vector pGL3-basic (Realgene, Nanjing, China). The recombinant plasmids were transfected into HGC27 and AGS cells with miR-622 mimic or miR-NC. After 48h, luciferase activity was determined under the VICTOR2 fluorometry (PerkinElmer, Waltham, MA, USA) and standardized to renilla luciferase activity.

EdU assay

Cell-Light EdU Apollo567 *In Vitro* Kit (RibiBio) was used to assess cell proliferation according to the kit

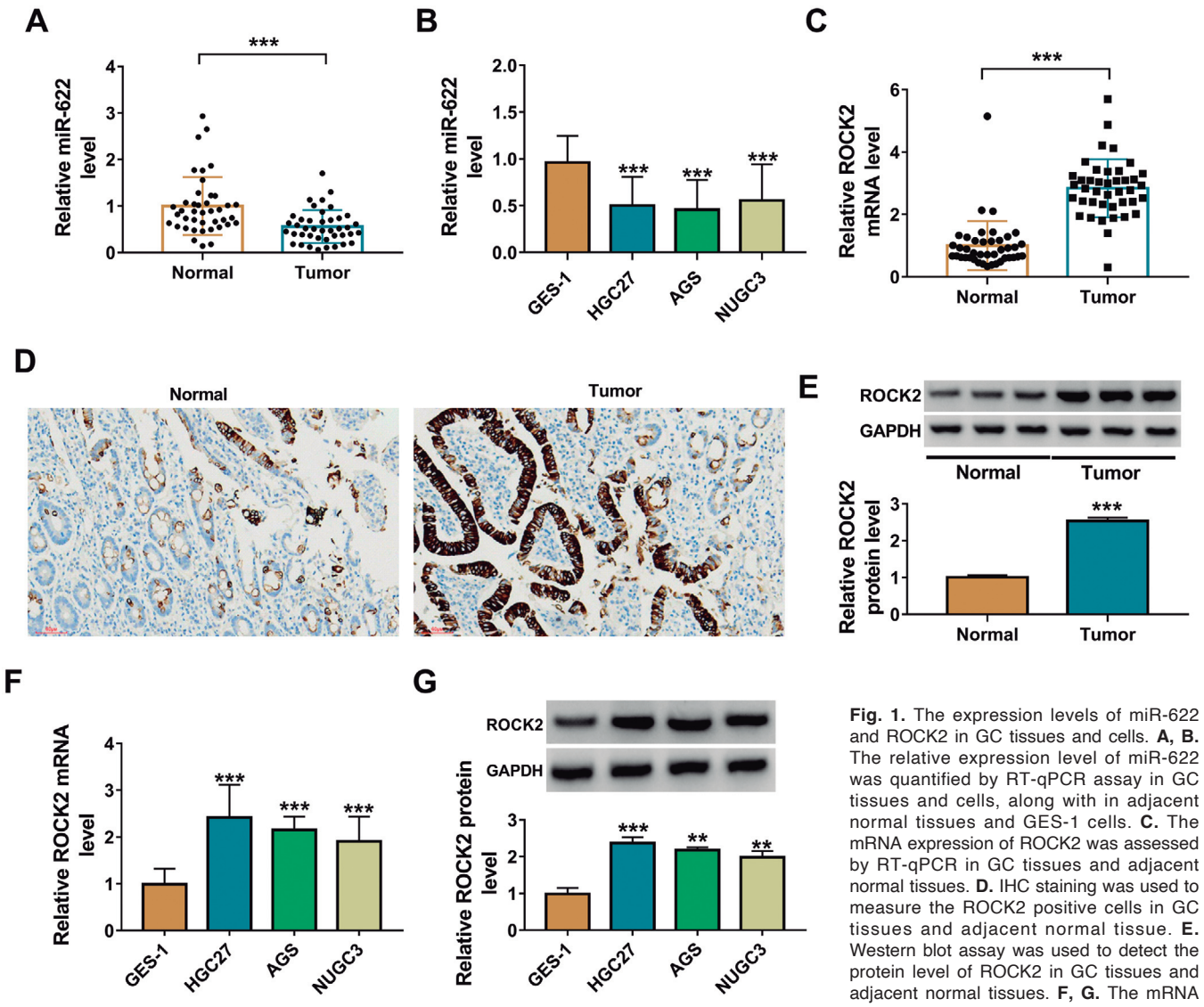

Fig. 1. The expression levels of miR-622 and ROCK2 in GC tissues and cells. **A, B.** The relative expression level of miR-622 was quantified by RT-qPCR assay in GC tissues and cells, along with in adjacent normal tissues and GES-1 cells. **C.** The mRNA expression of ROCK2 was assessed by RT-qPCR in GC tissues and adjacent normal tissues. **D.** IHC staining was used to measure the ROCK2 positive cells in GC tissues and adjacent normal tissue. **E.** Western blot assay was used to detect the protein level of ROCK2 in GC tissues and adjacent normal tissues. **F, G.** The mRNA and protein expression of ROCK2 in GC cells and GES-1 cells was determined by RT-qPCR and western blot assay. ***P*<0.01, ****P*<0.001.

instructions. Cell fluorescence was observed with a fluorescence microscope (Mshot, Guangdong, China; 100×), and Image J software was used to analyze the EdU positive cells.

Colony-forming assay

HGC27 and AGS cells were seeded into 6-well plates (1000 cells/well) and incubated for 14 days to allow them to form colonies. Then colonies were fixed with 95% ethanol and then stained with 0.5% crystal violet solution (Beyotime) for 20 min. After that, the colonies were then counted under an inverted microscope (Mshot).

Cell apoptosis assay

In brief, HGC27 and AGS cells were washed by PBS and then collected by trypsin after transfection 48h. The single cell suspension (1×10^6/mL) was fixed in 95% ethanol and then stained with staining buffer containing Annexin V-FITC and PI (BestBio, Shanghai, China) for 20 min in dark conditions. Finally, apoptotic cells were monitored under flow cytometry (Becton Dickinson, San Jose, CA, USA).

Migration and invasion assay

The 24-well transwell chamber (8-μm pore size; Corning, Franklin Lakes, NJ, USA) was used to test cells migration. HGC27 and AGS cells (1×10^5/mL) were re-suspended in 200 μL of medium without FBS and then added into the upper chamber. Following a 48h cultivation, cells that invaded to the lower chamber were fixed in 95% ethanol methanol and stained with 0.1% crystal violet (Beyotime). Finally, representative pictures were photographed under the microscope (Mshot; 100×), and Image J software was used for data analysis. In addition, the upper chamber was covered with matrigel (Becton Dickinson) for invasion assay.

RNase R assay and Actinomycin D (Act D) assay

The RNA extracted from HGC27 and AGS cells was incubated with or without RNase R (Geneseed, Guangzhou, China) followed by RT-qPCR to measure the circ_0000467 expression and linear RNA SKA mRNA expression. In addition, HGC27 and AGS cells were incubated with Act D solution (Millipore, Billerica, MA, USA), and the circ_0000467 expression and linear RNA SKA mRNA expression were analyzed by RT-qPCR.

RIP assay

Based on the instructions of Magna RIP Kit (Millipore), HGC27 and AGS cells were treated with RIP lysis buffer, and then the cell extracts were mixed with magnetic beads pre-coated anti-IgG or anti-AGO2. The enrichments of circ_0000467 and miR-633 were

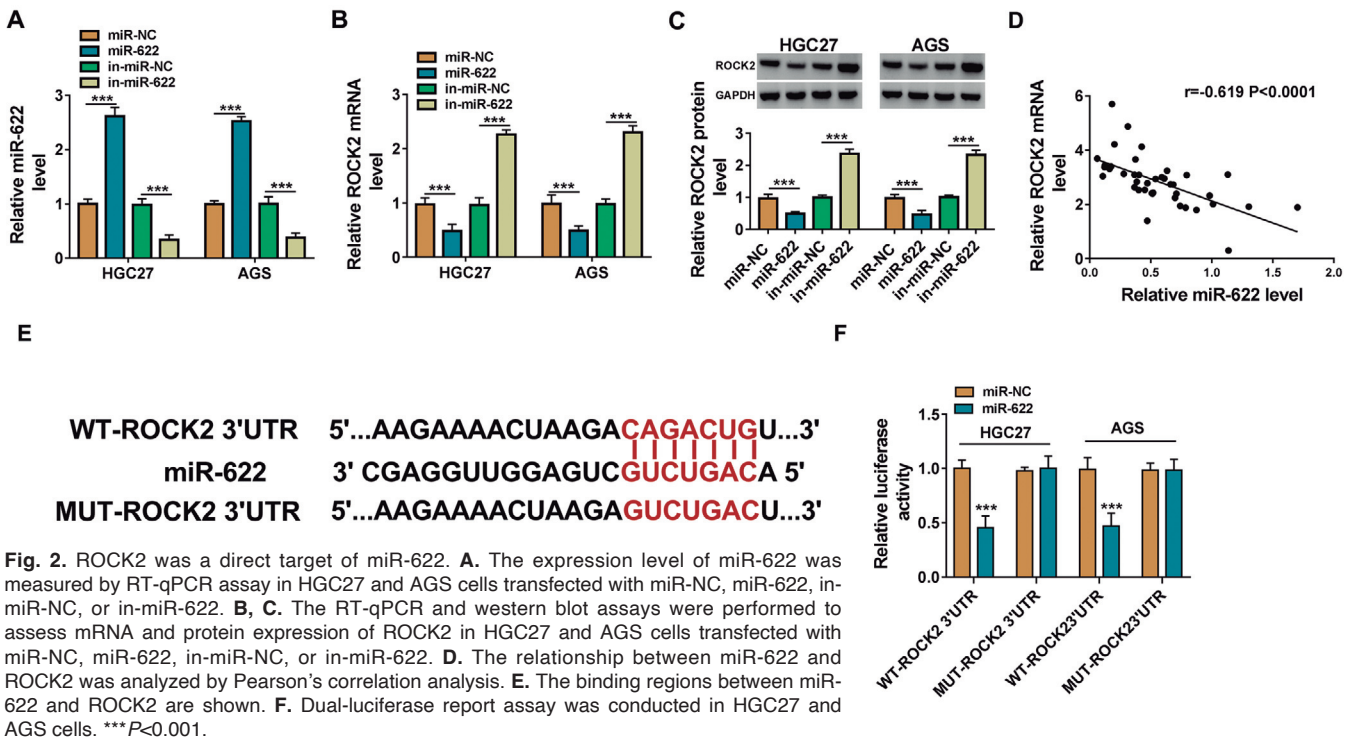

Fig. 2. ROCK2 was a direct target of miR-622. **A.** The expression level of miR-622 was measured by RT-qPCR assay in HGC27 and AGS cells transfected with miR-NC, miR-622, in-miR-NC, or in-miR-622. **B, C.** The RT-qPCR and western blot assays were performed to assess mRNA and protein expression of ROCK2 in HGC27 and AGS cells transfected with miR-NC, miR-622, in-miR-NC, or in-miR-622. **D.** The relationship between miR-622 and ROCK2 was analyzed by Pearson's correlation analysis. **E.** The binding regions between miR-622 and ROCK2 are shown. **F.** Dual-luciferase report assay was conducted in HGC27 and AGS cells. ***P<0.001.

quantified by RT-qPCR.

In vivo experiment

BALB/C athymic nude mice (Vital River Laboratory, Beijing, China) were randomly divided into two groups (n=6 in each group). HGC27 cells stably transfected with sh-circ_0000467 (RiboBio) or sh-NC were hypodermically injected into the left flank of the nude mice (5×10^6 cells/100 μL PBS/mice). Four weeks later, mice were euthanized by flowing CO_2, and tumors tissues were collected for analysis. In addition, a part of the fresh tissue was prepared into paraffin sections, and then the tissue was stained. IHC staining was performed using ROCK2 antibody (#9029S; 1:50 dilution, CST) and Ki-67 antibody (#9449; 1:200 dilution, CST) and SP kit. In addition, tumor growth was monitored every week using volume=1/2 (length× width^2). Animal experiments strictly obeyed the instruction of the Institutional Animal Care and Use Committee of the central hospital of enshi tujia and miao autonomous prefecture.

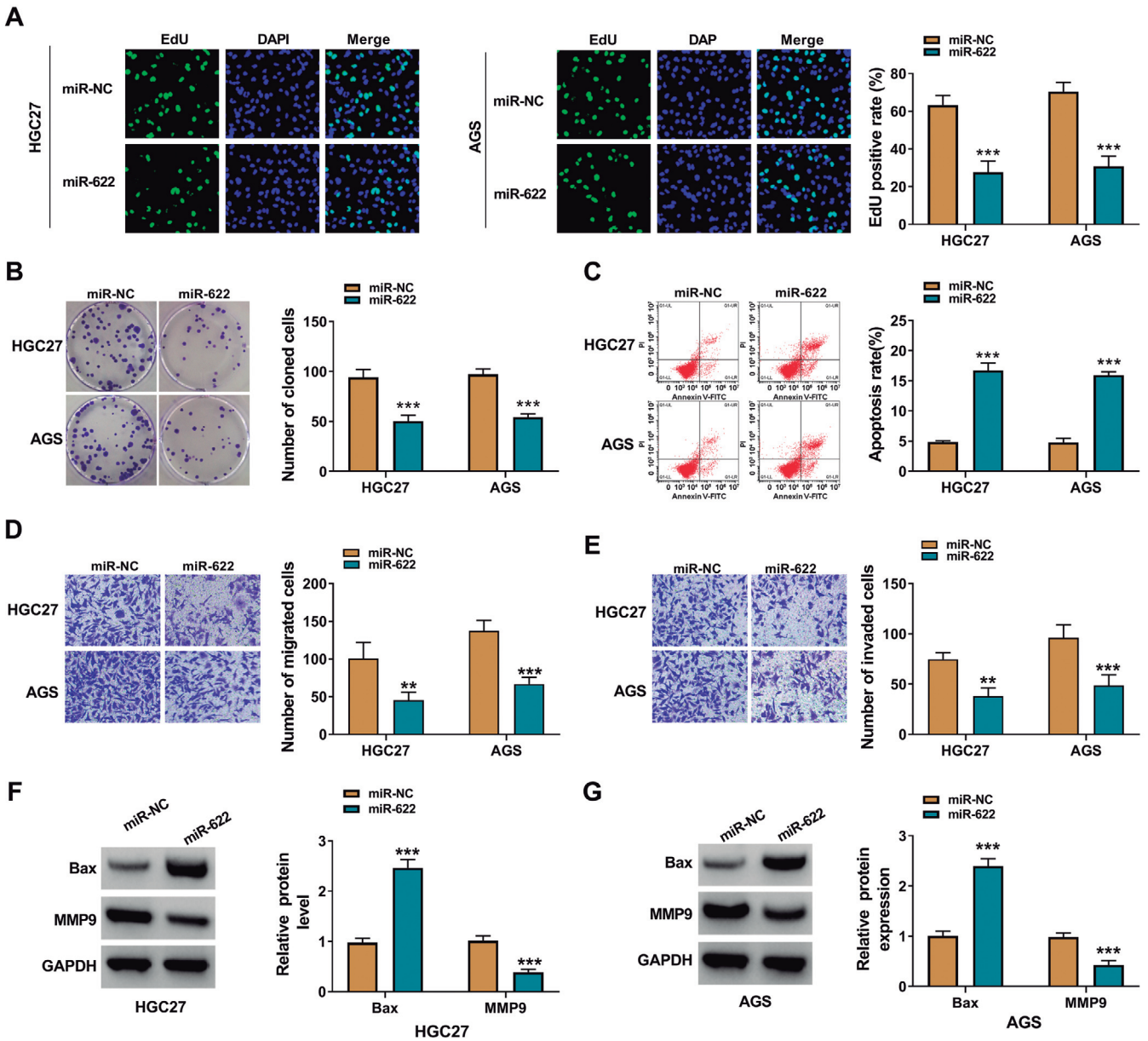

Fig. 3. Influences of miR-622 overexpression on proliferation, migration, invasion, and apoptosis of GC cells. **A-G.** HGC27 and AGS cells were transfected with miR-NC or miR-622. The proliferation of HGC27 and AGS cells was analyzed by EdU staining **(A)** and colony-forming assay **(B)**. **C.** The apoptotic cells were distinguished by flow cytometry assay. **D, E.** Transwell assay was employed to measure the migration and invasion of HGC27 and AGS cells. **F, G.** The protein expression levels of Bax and MMP9 were quantified by western blot assay. ***P*<0.01, ****P*<0.001.

Statistical analysis

SPSS 21.0 software (IBM, Somers, NY, USA) was used for statistical analysis, and all data were exhibited as mean ± standard deviation. The Student's 2-tailed t-test was used for comparisons of two treatment groups, while one-way analysis of variance was used for multiple groups. The differences were considered to be significant at $P<0.05$. Pearson's correlation analysis was used to determine association among circ_0000467, miR-622, and ROCK2.

Results

MiR-622 was decreased and ROCK2 was increased in GC tissues and cells

As presented in Fig. 1A,B, the results of RT-qPCR assay suggested that miR-622 was downregulated in GC tissues compared with paired neighboring normal tissues; besides, GC cells showed a lower expression of miR-622 than control cells. Furthermore, ROCK2 was obviously increased in GC tissues compared with adjacent normal tissues (Fig. 1C). IHC staining results confirmed that the ROCK2 positive cells were enhanced in GC tissues (Fig. 1D). At the protein level, ROCK2 also was found to be highly expressed in GC tissues (Fig. 1E). In addition, ROCK2 was more highly expressed in GC cells (HGC27, AGS and NUGC3) than in GES-1 cells at the mRNA level and protein level (Fig. 1F,G). Thus the roles of miR-622 and ROCK2 were explored in GC.

ROCK2 was a direct target of miR-622 in GC cells

The possible regulatory relationship between miR-622 and ROCK2 was investigated in HGC27 and AGS cells. In transfection experiments, miR-622 was upregulated in cells transfected with miR-622 mimic while it was downregulated in HGC27 and AGS cells transfected with in-miR-622 (Fig. 2A). Importantly, overexpression of miR-622 decreased ROCK2, while a shortage of miR-622 increased ROCK2 expression in GC cells (Fig. 2B,C). We also noticed that miR-622 was negatively correlated with ROCK2 expression in GC tissues (Fig. 2D). We hypothesized that ROCK2 was a target of miR-622. As shown in Fig. 2E, miR-622 had the binding sites with the 3'UTR of ROCK2. Through dual-luciferase reporter assay, we found that miR-622 mimic could reduce the luciferase activity of WT-ROCK2 3'UTR vector without affecting the luciferase activity of MUT-ROCK2 3'UTR vector (Fig. 2F). These data suggested that miR-622 targeted ROCK2 expression in GC cells.

Overexpression of miR-622 inhibited proliferation, migration, and invasion while it increased apoptosis of GC cells

The regulatory roles of miR-622 were investigated in HGC27 and AGS cells after transfection with miR-622 mimic. EdU assay, colony-forming assay and flow cytometry results showed that the upregulation of miR-622 significantly decreased proliferation and induced apoptosis of HGC27 and AGS cells (Fig. 3A-C). The overexpression of miR-622 also resulted in the significant decrease on migration and invasion of GC cells (Fig. 3D,E). The western blot analysis was used to show Bax and MMP9 levels in HGC27 and AGS cells. Overexpression of miR-622 increased Bax while it decreased MMP9 expression (Fig. 3F,G). In summary, miR-622 played key roles in proliferation, migration,

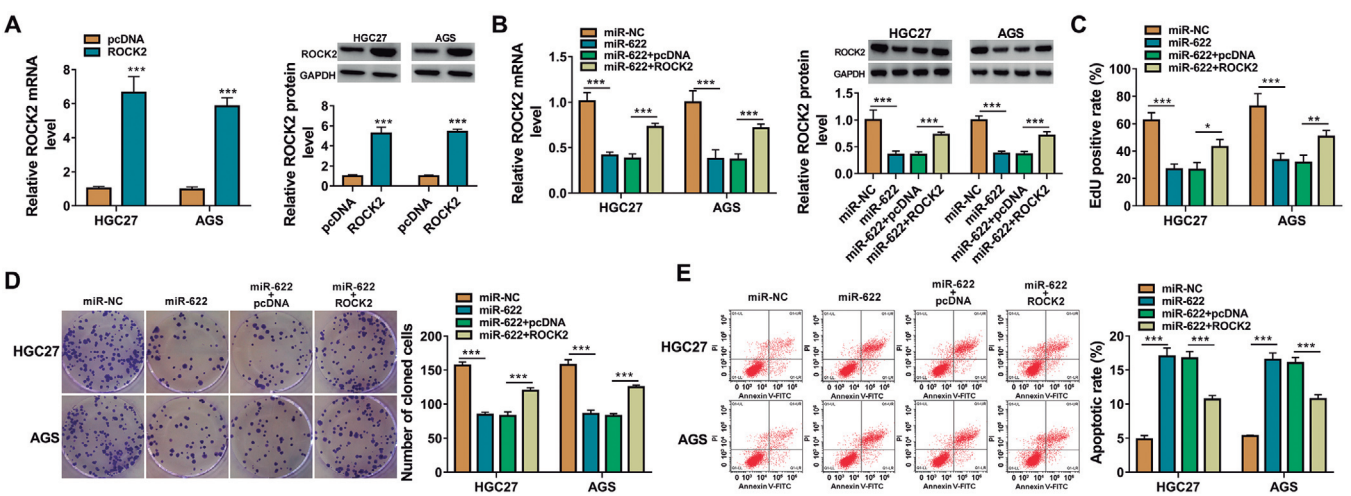

Fig. 4. MiR-622 regulated proliferation and apoptosis of GC cells by targeting ROCK2. **A.** The overexpression efficiency of pcDNA ROCK2 overexpression vector was confirmed by RT-qPCR assay. **B-E.** HGC27 and AGS cells were transfected with miR-NC, miR-622, miR-622+pcDNA, or miR-622+ROCK2. **B.** The expression level of ROCK2 was determined by RT-qPCR and western blot assays. EdU assay **(C)** and colony-forming assay **(D)** were used to determine the proliferation of HGC27 and AGS cells. **E.** The flow cytometry assay was performed in transfected HGC27 and AGS cells. **P*<0.05, ***P*<0.01, ****P*<0.001.

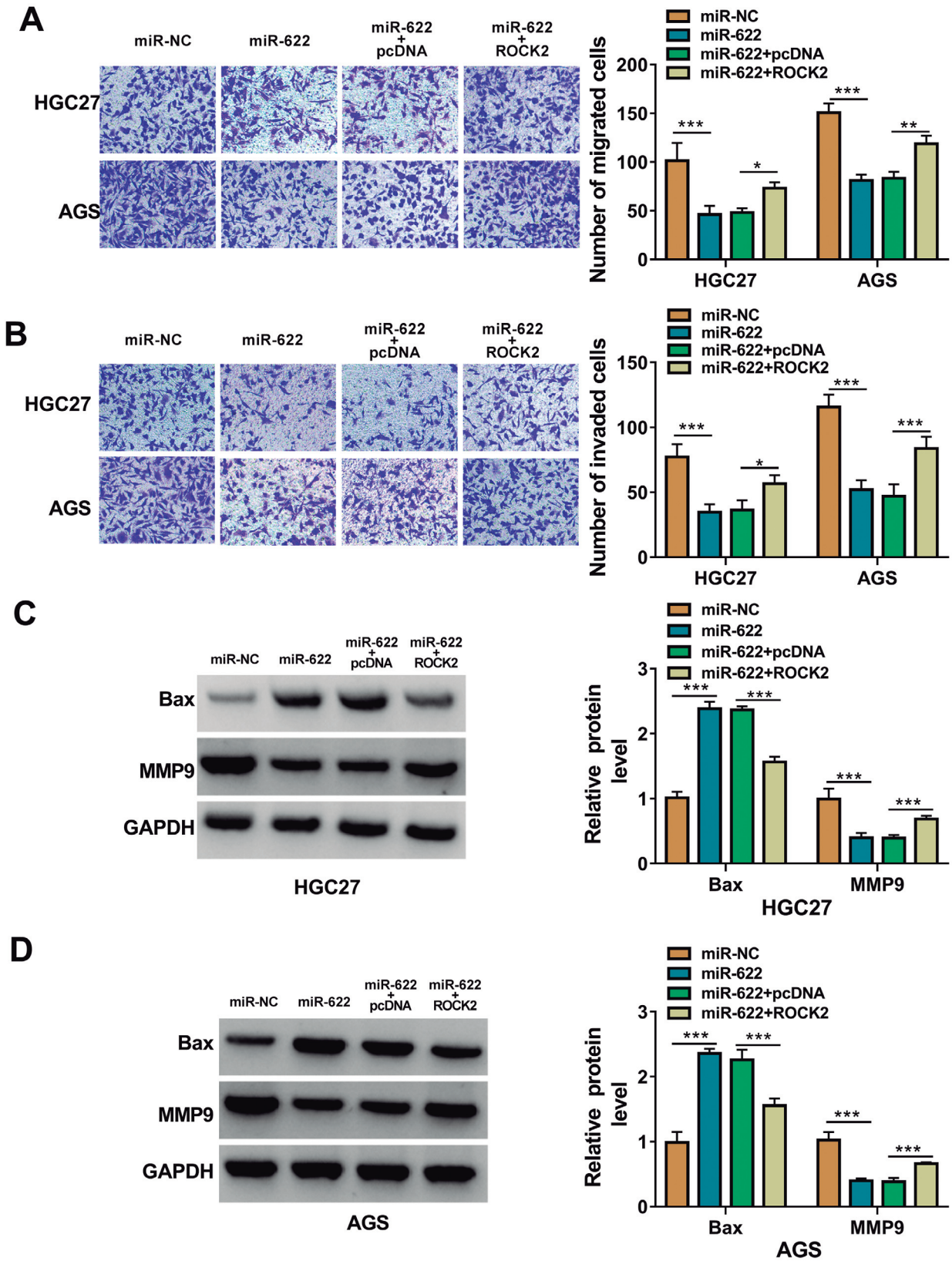

Fig. 5. MiR-622 targeted ROCK2 to regulate GC cell migration and invasion. HGC27 and AGS cells were transfected with miR-NC, miR-622, miR-622+pcDNA, or miR-622+ROCK2. **A, B.** The migration and invasion of HGC27 and AGS cells were assessed by transwell assay. **C, D.** The western blot assay was used to measure protein expression levels of Bax and MMP9. **P*<0.05, ***P*<0.01, ****P*<0.001.

invasion, and apoptosis of GC cells.

Overexpression of ROCK2 reversed miR-622-induced effects on GC cells.

The underlying mechanism by which miR-622 regulated proliferation, migration, invasion, and apoptosis in GC cells was analyzed. We found that the mRNA and protein expression of ROCK2 was overexpressed in HGC27 and AGS cells after transfection with pcDNA ROCK2 overexpression vector (Fig. 4A). In HGC27 and AGS cells co-transfected with miR-622 mimic and ROCK2 overexpression vector, we found that ROCK2 overexpression vector also eliminated the decreasing effect of miR-622 mimic on ROCK2 mRNA and protein expression (Fig. 4B). Through detecting EdU positive cells and the number of cloned cells, we confirmed that the inhibitory effect on cell proliferation induced by miR-622 overexpression was abolished by upregulation of ROCK2 (Fig. 4C,D). The overexpression of ROCK2 protected HGC27 and AGS cells from miR-622-induced apoptosis (Fig. 4E). A significant decrease of migration and invasion was observed in miR-622-overexpressed HGC27 and AGS cells, which was abolished by overexpression of ROCK2 (Fig. 5A,B). Furthermore, elevating miR-622 expression increased Bax while decreased MMP9 expression, which it was overturned by upregulation of ROCK2 (Fig. 5C,D). Therefore, miR-622 regulated proliferation, migration, invasion, and apoptosis by targeting ROCK2 in GC cells.

Circ_0000467 targeted miR-622 in GC cells

Circ_0000467 is located at chr13 and is derived from the SKA3 gene (Fig. 6A). Compared to linear RNA SKA3, we found that circ_0000467 was resistant to RNase R digestion and not affected by Act D with high stability (Fig. 6B,C). The expression level of circ_0000467 was measured in GC tissues and cells and the results showed that circ_0000467 was obviously upregulated in GC tissues and cells compared with controls (Fig. 6D,E). Importantly, circ_0000467 was downregulated in si-circ_0000467 group compared with si-NC group (Fig. 6F). Interestingly, silencing of circ_0000467 enhanced the expression of miR-622 in HGC27 and AGS cells (Fig. 6G). A negative correlation between circ_0000467 and miR-622 was found in GC

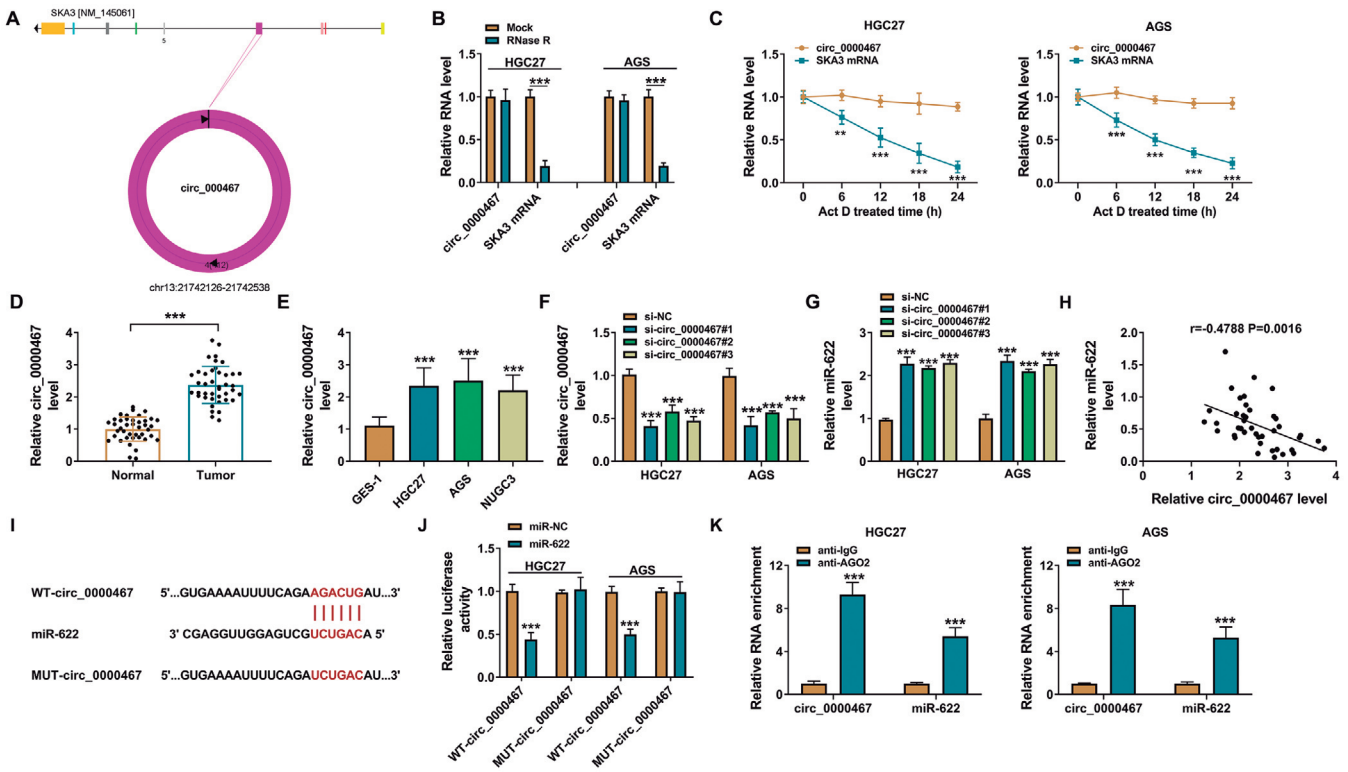

Fig. 6. MiR-622 was a target of circ_0000467. **A.** The basic information of circ_0000467 is shown. RNase R assay **(B)** and Act D assay **(C)** were used to assess the circular characteristics of circ_0000467. **D, E.** The RT-qPCR assay was carried out to examine circ_0000467 level in GC tissues and cells. **F, G.** The expression of circ_0000467 and miR-622 was examined by RT-qPCR assay in HGC27 and AGS cells transfected with si-NC, si-circ_0000467#1, si-circ_0000467#2, or si-circ_0000467#3. **H.** The relationship between circ_0000467 and miR-622 was analyzed. **I.** The complementary sequences between circ_0000467 and miR-622 are shown. Dual-luciferase reporter assay **(J)** and RIP assay **(K)** were introduced to confirm the interaction between circ_0000467 and miR-622. ***P*<0.01, ****P*<0.001.

tissues (Fig. 6H). The possible complementary sequences between circ_0000467 and miR-622 are shown in Fig. 6I. Moreover, dual-luciferase reporter experiment revealed the interacting relationship between circ_0000467 and miR-622, showing decreasing luciferase activity in HGC27 and AGS cells co-

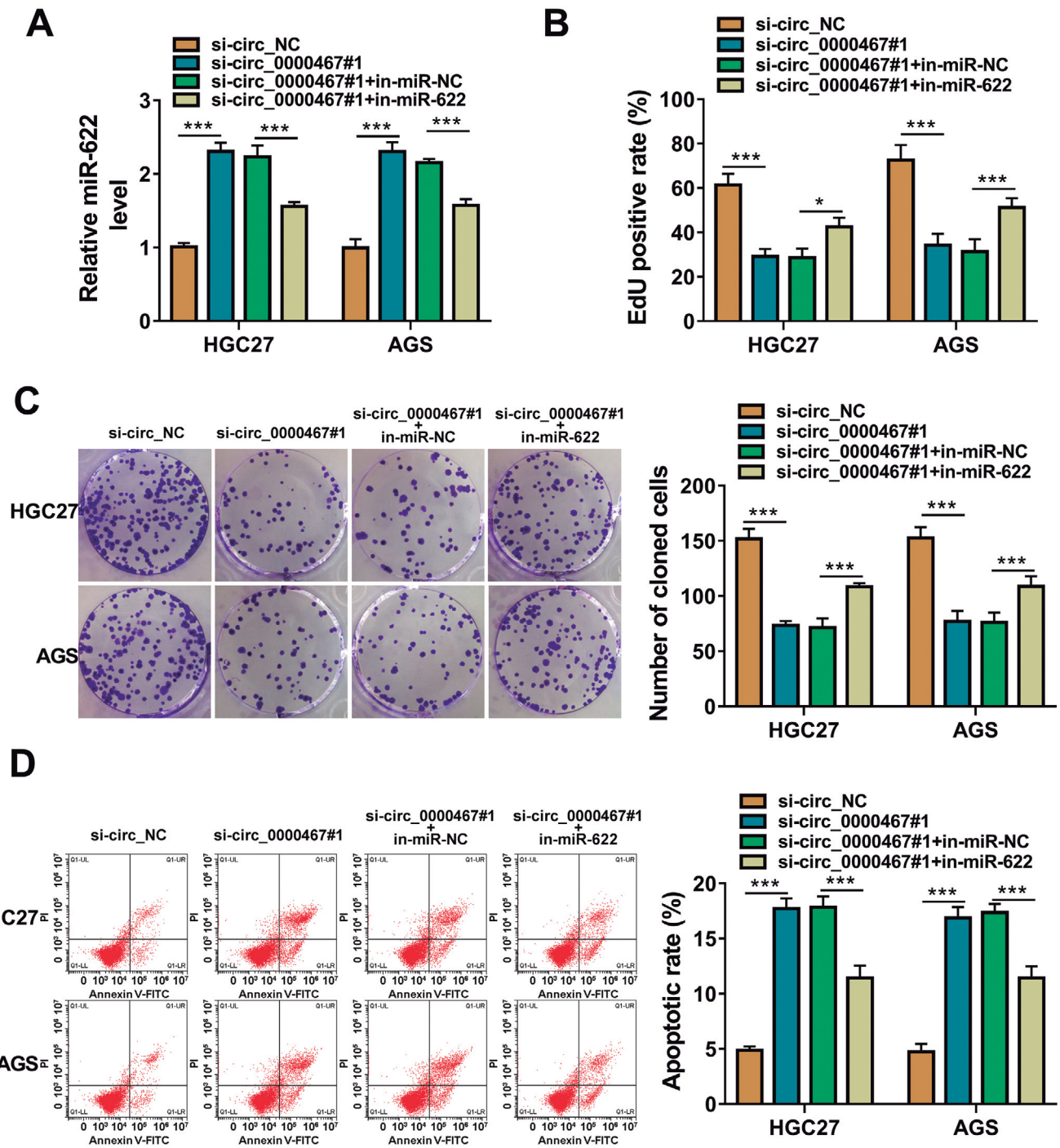

Fig. 7. Knockdown of miR-622 partially reversed the si-circ_0000467-induced effects on GC cell proliferation and apoptosis. HGC27 and AGS cells were infected with si-NC, si-circ_0000467#1, circ_0000467#1+in-miR-NC, or circ_0000467#1+in-miR-622. **A.** The expression of miR-622 was assessed by RT-qPCR assay. EdU assay **(B)** and colony-forming assay **(C)** were performed to measure the proliferation of cells. **D.** The flow cytometry assay was conducted to assess cell apoptosis. **P*<0.05, ****P*<0.001.

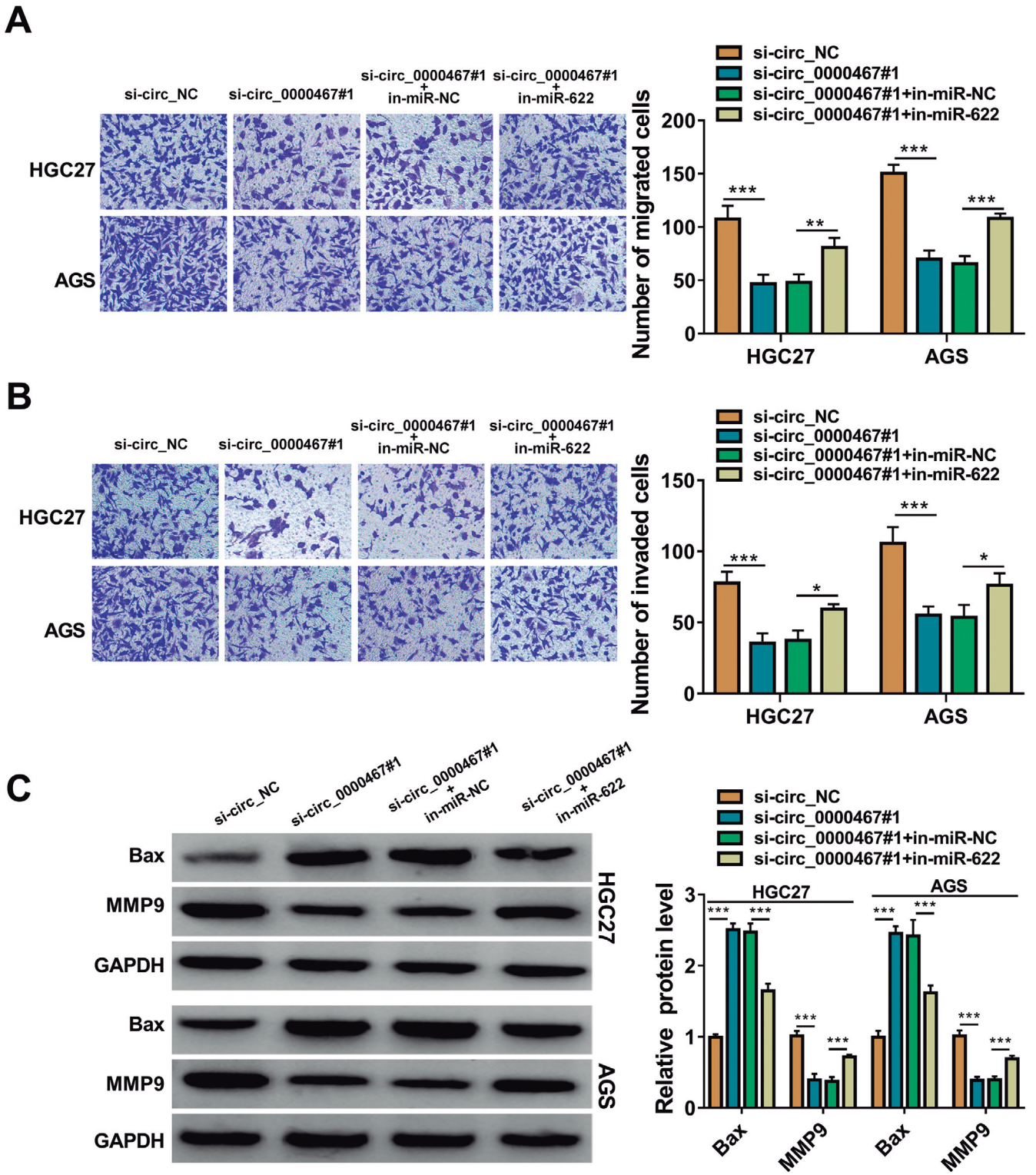

Fig. 8. Knockdown of miR-622 partially reversed the si-circ_0000467-induced effects on GC cell migration and invasion. HGC27 and AGS cells were infected with si-NC, si-circ_0000467#1, circ_0000467#1+in-miR-NC, or circ_0000467#1+in-miR-622. **A, B.** The migration and invasion were determined by transwell assay. **C.** The expression of Bax and MMP9 was analyzed by western blot assay. **P*<0.05, ***P*<0.01, ****P*<0.001.

transfected with miR-622 mimic and WT-circ_0000467 vector (Fig. 6J). In addition, the results of RIP assay revealed that circ_0000467 and miR-622 were markedly enriched in anti-AGO2 (Fig. 6K). The above results indicated that miR-622 was a target of circ_0000467.

Circ_0000467 regulated proliferation, migration, invasion, and apoptosis of GC cells by targeting miR-622

To further elucidate whether circ_0000467 targeted miR-622 to regulate proliferation, migration, invasion, and apoptosis of GC cells, a functional experiment was performed. The upregulation of miR-622 in si-circ_0000467 transfected cells was reversed by transfection with miR-622 inhibitor (Fig. 7A). EdU assay and colony-forming assay revealed that cell proliferation was significantly suppressed by si-circ_0000467 transfection, while co-transfection with miR-622 inhibitor mitigated this effect in HGC27 and AGS cells (Fig. 7B,C). The promotive effects of circ_0000467 silencing on cell apoptosis was abolished by silencing of miR-622 (Fig. 7D). The depletion of miR-622 successfully restored si-circ_0000467-induced inhibitory effects on migration and invasion of GC cells (Fig. 8A,B). Suppression of circ_0000467 increased Bax while it decreased MMP9 expression, which was reversed by downregulation of miR-622 (Fig. 8C). These findings confirmed that silencing of miR-622 partially reversed si-circ_0000467-induced effects on GC cells.

Inhibition of circ_0000467 inhibited tumor growth

As presented in Figure 9A,B, si-circ_0000467-induced downregulation of ROCK2 was abolished by inhibition of miR-622. To validate the suppressive activity of circ_0000467 silencing on GC tumors, a xenograft experiment in nude mice was performed. Inhibition of circ_0000467 decreased the volume and weight of tumor tissues compared with control group (Fig. 9C,D). In addition, circ_0000467 and ROCK2 were decreased and miR-622 was increased in sh-circ_0000467 group compared to the sh-NC group (Fig. 9E-H). IHC staining results showed that Ki-67 positive cells and ROCK2 positive cells were reduced in the tumor tissues of the sh-circ_0000467 group (Fig. 9I). To conclude, inhibition of circ_0000467 inhibited tumor growth partially by regulation of miR-622 and ROCK2.

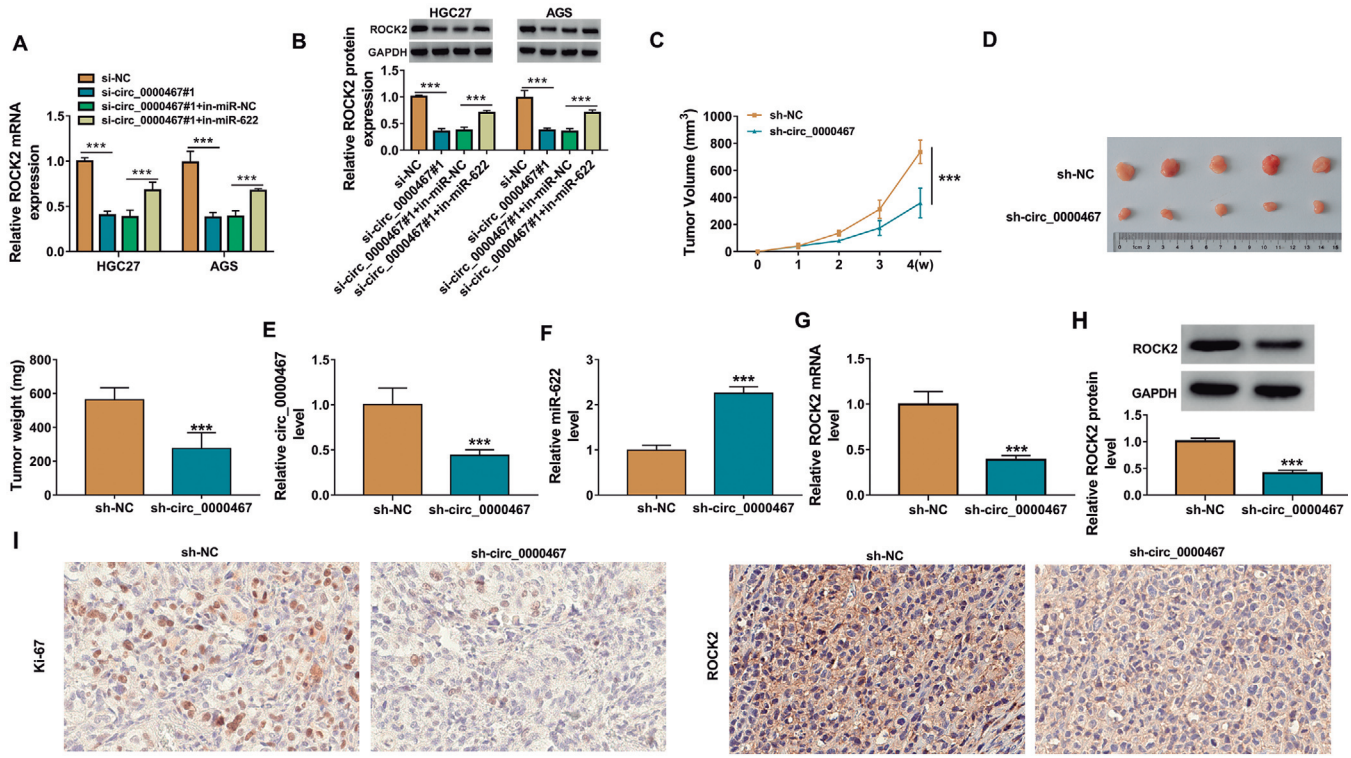

Fig. 9. Silencing of circ_0000467 inhibited tumor growth *in vivo* by regulation of miR-622 and ROCK2. **A, B.** The expression level of ROCK2 was calculated by RT-qPCR and western blot assays in HGC27 and AGS cells transfected with si-NC, si- circ_0000467#1, circ_0000467#1+in-miR-NC, or circ_0000467#1+in-miR-622. **C, D.** The growth curves and weights of xenograft tumors are shown. **E-G.** The expression levels of circ_0000467, miR-622, and ROCK2 were estimated with RT-qPCR assay. **H.** Western blot assay was performed to test the expression of ROCK2, with GAPDH as control. **I.** IHC staining was performed to assess the Ki-67 positive cells and ROCK2 positive cells in the tumor tissues of each group. ***P<0.001.

Discussion

To conclude, current data indicated that circ_0000467 was upregulated in GC. Abundant evidence has demonstrated that circRNAs played vital roles in GC (Li et al., 2020). The prognostic significance of circ_0000467 was revealed in GC by Lu et al. (2019). As we expected, the potential carcinogenic functional effects of circ_0000467 was also identified in our results. In addition, previous studies have demonstrated that circRNAs functioned as competitive endogenous RNAs (ceRNAs) to sponge to miRNA, thereby regulating target gene expression (Kristensen et al., 2019). Mo et al. reported that circ_0000467 affected the growth and migration of GC cells by sponging miR-326-3p (Mo et al., 2020). Analogously, our data indicated that circ_0000467 regulated cell growth, movement, and apoptosis of GC cells by targeting the miR-622/ROCK2 axis.

The tumor inhibitory roles of miR-622 were found in hepatocellular carcinoma (Song et al., 2015). Not surprisingly, Guo et al. also observed that decreased expression of miR-622 promoted migration and invasion of GC cells (Guo et al., 2011). Additionally, identification of downstream target mRNA is of importance in deciphering the function of miR-622 in GC. Several lines of evidence indicated that miR-622 displayed a suppressive effect on colorectal cancer process via targeting of the kirsten rat sarcoma (K-Ras) gene (Fang et al., 2016). Knockdown of miR-622 was able to facilitate GC invasion and metastasis (Guo et al., 2011). In line with the above reports, our results also suggested that miR-622 acted as an inhibitor gene in GC by regulating ROCK2 expression.

It is commonly thought that the important function of miRNAs is to target 3'UTR of mRNA, thereby regulating gene-expression post-transcriptionally (Towler et al., 2015). ROCK2 has been documented to be increased in multiple types of malignant tumors, and it is targeted by multiple miRNAs, such as miR-185-5p (Niu and Tang, 2019), miR-455-3p (Wu et al., 2018), and miR-144 (Wang et al., 2015). ROCK2 has been identified to contribute to tumor development and progression in GC (Li et al., 2017; Xie et al., 2019; Wang et al., 2020). Consistently, our results also suggested that overexpression of ROCK2 promoted the development of GC. In addition, the tumor-promoting activity of ROCK2 has been found to be associated with activation of Rho/Rho-associated protein kinases (ROCK) signaling (Liu et al., 2019b). Increased activity of ROCK signaling was well documented in GC and related to motility and metastasis of GC (Matsuoka and Yashiro, 2014). According to a previous report, targeting ROCK signaling might be a reliable strategy for GC treatment (Xu et al., 2012).

In summary, our study focused on the regulatory effects of circ_0000467 in GC and partially revealed the underlying molecular mechanisms associated with miR-622 and ROCK2, highlighting new perspectives on the roles of circ_0000467 in GC.

Conclusion

Collectively, the present study demonstrated that circ_0000467/miR-622/ROCK2 axis played a crucial role in GC, and inhibition of circ_0000467 suppressed proliferation, migration, and invasion while it induced apoptosis of GC by functioning as a sponge for miR-622 to upregulate ROCK2 expression. This will be helpful for further understanding the regulatory mechanisms of circ_0000467 in GC.

Acknowledgements. None.

Ethics approval and consent to participate. Written informed consent was obtained from patients with approval by the Institutional Review Board in The Central Hospital of Enshi Tujia and Miao Autonomous Prefecture.

Consent for publication. Not applicable.

Availability of data and materials. Please contact the correspondence author for data request.

Competing interests. The authors declare that they have no conflicts of interest.

Funding. None.

Authors' contribution. Shengquan Tan had full access to all of the data in the study and takes responsibility for the integrity of the data and the accuracy of the data analysis. Study concept and design: Shengquan Tan, Lingbo Hu and Rui Lei; acquisition of data: Shengquan Tan, Ruo Wang and Jiaquan Chen; critical revision of the manuscript for important intellectual content: Shengquan Tan, Lingbo Hu and Rui Lei; administrative, technical or material support: Shengquan Tan, Rui Lei, Ruo Wang and Jiaquan Chen; study supervision: Shengquan Tan.

References

Bray F., Ferlay J., Soerjomataram I., Siegel R.L., Torre L.A. and Jemal A. (2018). Global cancer statistics 2018: Globocan estimates of incidence and mortality worldwide for 36 cancers in 185 countries. CA Cancer J. Clin. 68, 394-424.

Correa P. (2013). Gastric cancer: Overview. Gastroenterol. Clin. North Am. 42, 211-217.

Fang Y, Sun B, Li Z, Chen Z and Xiang J. (2016). MiR-622 inhibited colorectal cancer occurrence and metastasis by suppressing K-Ras. Mol. Carcinog. 55, 1369-1377.

Fang Y., Sun B., Wang J. and Wang Y. (2019). Mir-622 inhibits angiogenesis by suppressing theCXCR4-VEGFA axis in colorectal cancer. Gene 699, 37-42.

Guo X.B., Jing C.Q., Li L.P., Zhang L., Shi Y.L., Wang J.S., Liu J.L. and Li C.S. (2011). Down-regulation of miR-622 in gastric cancer promotes cellular invasion and tumor metastasis by targeting ING1 gene. World J. Gastroenterol. 17, 1895-1902.

Julian L. and Olson M.F. (2014). Rho-associated coiled-coil containing kinases (ROCK): Structure, regulation, and functions. Small GTPases 5, e29846.

Kristensen L.S., Andersen M.S., Stagsted L.V.W., Ebbesen K.K., Hansen T.B. and Kjems J. (2019). The biogenesis, biology and characterization of circular RNAs. Nat. Rev. Genet. 20, 675-691.

Li M., Ke J., Wang Q., Qian H,. Yang L., Zhang X., Xiao J., Ding H.,

Shan X., Liu Q., Xiao Y., Bao B. and Huang H. (2017). Upregulation of ROCK2 in gastric cancer cell promotes tumor cell proliferation, metastasis and invasion. Clin. Exp. Med. 17, 519-529.

Li R., Jiang J., Shi H., Qian H., Zhang X. and Xu W. (2020). CircRNA: A rising star in gastric cancer. Cell. Mol. Life Sci. 77, 1661-1680.

Liu C., Min L., Kuang J., Zhu C., Qiu X.Y. and Zhu L. (2019a). Bioinformatic identification of mir-622 key target genes and experimental validation of the miR-622-RNF8 axis in breast cancer. Front. Oncol. 9, 1114.

Liu J., Yang X., Shen K., Zeng L. and Sun Y. (2019b). [chloroxoquinoline inhibits invasion in breast cancer via down-regulating rho/rho kinase signaling pathway]. Zhejiang Da Xue Xue Bao. Yi Xue Ban Med. Sci. 48, 631-637 (in Chinese).

Lu J., Zhang P.Y., Xie J.W., Wang J.B., Lin J.X., Chen Q.Y., Cao L.L., Huang C.M., Li P. and Zheng C.H. (2019). Hsa_circ_0000467 promotes cancer progression and serves as a diagnostic and prognostic biomarker for gastric cancer. J. Clin. Lab. Anal. 33, e22726.

Lu J., Wang Y.H., Yoon C., Huang X.Y., Xu Y., Xie J.W., Wang J.B., Lin J.X., Chen Q.Y., Cao L.L., Zheng C.H., Li P. and Huang C.M. (2020). Circular RNA circ-RanGAP1 regulates VEGFA expression by targeting miR-877-3p to facilitate gastric cancer invasion and metastasis. Cancer Lett. 471, 38-48.

Matsuoka T and Yashiro M. (2014). Rho/ROCK signaling in motility and metastasis of gastric cancer. World J. Gastroenterol. 20, 13756-13766.

Mo W.L., Jiang J.T., Zhang L., Lu Q.C., Li J., Gu W.D., Cheng Y. and Wang H.T. (2020). Circular RNA hsa_circ_0000467 promotes the development of gastric cancer by competitively binding to microrRNA miR-326-3p. BioMed Res. Int. 2020, 4030826.

Niu Y. and Tang G. (2019). MiR-185-5p targets ROCK2 and inhibits cell migration and invasion of hepatocellular carcinoma. Oncol. Lett. 17, 5087-5093.

Saliminejad K., Khorram Khorshid H.R., Fard S.S. and Ghaffari S.H. (2019). An overview of microrna: Biology, functions, therapeutics, and analysis methods. J. Cell. Physiol. 234, 5451-5465.

Song W.H., Feng X.J., Gong S.J., Chen J.M., Wang S.M., Xing D.J., Zhu M.H., Zhang S.H. and Xu A.M. (2015). MicroRNA-622 acts as a tumor suppressor in hepatocellular carcinoma. Cancer Biol. Ther. 16, 1754-1763.

Song Z., Wu Y., Yang J., Yang D. and Fang X. (2017). Progress in the treatment of advanced gastric cancer. Tumour Biol. 39, 1010428317714626.

Sun X., Zhang X., Chen S., Fan M., Ma S. and Zhai H. (2019). Myosin heavy chain-associated rna transcripts promotes gastric cancer progression through the miR-4529-5p/ROCK2 axis. Dig. Dis. Sci. 64, 3539-3548.

Towler B.P., Jones C.I. and Newbury S.F. (2015). Mechanisms of regulation of mature miRNAs. Biochem. Soc. Trans. 43, 1208-1214.

Wang D., Jiang X., Liu Y., Cao G., Zhang X. and Kuang Y. (2020). Circular RNA circ_HN1 facilitates gastric cancer progression through modulation of the miR-302b-3p/ROCK2 axis. Mol. Cell. Biochem. 476, 199-212.

Wang W., Zhou X. and Wei M. (2015). MicroRNA-144 suppresses osteosarcoma growth and metastasis by targeting ROCK1 and ROCK2. Oncotarget 6, 10297-10308.

Wei L., Surma M., Shi S., Lambert-Cheatham N. and Shi J. (2016). Novel insights into the roles of Rho kinase in cancer. Arch. Immunol. Ther. Exp. 64, 259-278.

Wu J., Liu J., Ding Y., Zhu M., Lu K., Zhou J., Xie X., Xu Y., Shen X., Chen Y., Shao X. and Zhu C. (2018). Mir-455-3p suppresses renal fibrosis through repression of ROCK2 expression in diabetic nephropathy. Biochem. Biophys. Res. Commun. 503, 977-983.

Xie Y., Qi J., Zhu C., Zhao D. and Liao G. (2019). MiR-381 functions as a tumor suppressor in gastric cancer by targeting ROCK2. Int. J. Clin. Exp. Pathol. 12, 164-172.

Xu X.T., Song Q.B., Yao Y., Ruan P. and Tao Z.Z. (2012). Inhibition of Rhoa/ROCK signaling pathway promotes the apoptosis of gastric cancer cells. Hepatogastroenterology 59, 2523-2526.

Xu J., Ma B., Chen G., Wei D., Li L. and Hu W. (2018). MicroRNA-622 suppresses the proliferation of glioma cells by targeting YAP1. J. Cell. Biochem. 119, 2492-2500.

Yi H., Wang K., Jin H., Su J., Zou Y., Li Q., He L., Liu X. and Du B. (2018). Overexpression of Rho-associated coiled-coil containing protein kinase 2 is correlated with clinical progression and poor prognosis in breast cancer. Med. Sci. Monit. 24, 4776-4781.

Accepted August 8, 2022